 doi:10.20944/preprints202006.0338.v1

Investigating the Effects of Cerebellar Transcranial Direct Current Stimulation on Post-Stroke Overground Gait Performance: a partial least-squares regression approach

Solanki, Dhaval[1*,#]; Rezaee, Zeynab[2,#]; Dutta, Anirban[2*,&]; Lahiri, Uttama[1,&]

[1]Electrical Engineering, Indian Institute of Technology Gandhinagar, Gujarat, India.

[2]Biomedical Engineering, University at Buffalo, New York, United States.

***Corresponding Authors:**

dhaval.solanki@iitgn.ac.in

anirband@buffalo.edu

[#] Junior authors equal contribution

[&] Senior authors equal contribution

Abstract

Stroke often results in impaired gait, which can limit community ambulation and the quality of life. Recent works have shown the feasibility of transcranial Direct Current Stimulation (tDCS) as an adjuvant treatment to facilitate gait rehabilitation. Since the cerebellum plays an essential role in balance and movement coordination, which is crucial for independent overground ambulation, so, we investigated the effects of cerebellar tDCS (ctDCS) on the post-stroke overground gait performance in chronic stroke survivors. Fourteen chronic post-stroke male subjects were recruited based on convenience sampling at the collaborating hospitals where ten subjects finally participated in the ctDCS study. We evaluated the effects of two ctDCS montages with 2mA direct current, a) optimized configuration for dentate stimulation with 3.14cm^2 disc anode at PO10h (10/5 EEG system) and 3.14cm^2 disc cathode at PO9h (10/5 EEG system), and b) optimized configuration for leg lobules VII-IX stimulation with 3.14cm^2 disc anode at Exx8 (electrodes defined by ROAST) and 3.14cm^2 disc cathode at Exx7. We found ctDCS to be acceptable by all the exposed subjects. The ctDCS intervention had an effect on the 'Normalised Step length Affected side' ($p=0.1$) and 'Gait Stability Ratio' ($p=0.0569$), which was found using Wilcoxon signed-rank test at 10% significance level. Also, ctDCS montage specific effect was found using a two-sided Wilcoxon rank-sum test at a 5% significance level for 'Step Time Affected Leg' ($p=0.0257$) and '%Stance Time Unaffected Leg' ($p=0.0376$). Moreover, the changes in the quantitative gait parameters across both the montages were found to be correlated to the mean electric field strength in the lobules based on partial least squares regression analysis (R^2 statistic = 0.6574) where the mean electric field strength at the cerebellar lobules, Vermis VIIIb, Ipsilesional IX, Vermis IX, Ipsilesional X, had the most loading. In

conclusion, our feasibility study indicated the potential of a single session of ctDCS to contribute to the immediate improvement in the balance and gait performance in terms of gait-related indices and clinical gait measures.

Keywords: Gait; Stroke; Cerebellum; Transcranial Direct Current Stimulation;

I. Background

Stroke is a leading cause of disability across the globe with 80·1 million (74·1 to 86·3) prevalent cases globally and 116·4 million (111·4 to 121·4) disability-adjusted life-years in 2016 [1]. Gait impairments occur in more than 80% of stroke survivors [2], where gait impairments remain in 25% of all stroke survivors despite rehabilitation [3]. However, the recovery of independent walking requires considerable practice in stroke survivors [4]. Conventional gait training can play an important role [4] besides assistive robotic devices and brain-computer interfaces where a combination may be more effective than over-ground gait training alone [5]. During such gait training, neuroplasticity can be facilitated with adjuvant treatment with non-invasive brain stimulation (NIBS) techniques to the lower limb motor cortex of stroke survivors [6]. Here, moderate-quality evidence has been found on NIBS combined with various therapies to improve gait speed after stroke [7], [8]. Importantly, NIBS treatment effects were found significant only in the care of transcranial magnetic stimulation (TMS), while transcranial direct current stimulation (tDCS) did not show any significant therapeutic effects [8]. Here, it is important to note that the tDCS effects are governed by various parameters, including current intensity, electrode size, electrode placement, that may affect the efficacy of stimulation and the therapeutic outcomes [9]. Furthermore, the specificity of the tDCS is challenging, especially for the leg representations in the primary motor cortex at the interhemispheric fissure, as demonstrated by Foerster et al. in healthy humans based on computational modeling and neurophysiological testing [10]. Such specificity is particularly relevant for post-stroke patients with hemiplegia who may have an imbalance in the inter-hemispheric inhibition after stroke [11].

Transcranial direct current stimulation (tDCS) [12] involves passing constant weak direct current (generally of the order of 1-2 mA) through one's scalp via a pair of electrodes (anode and cathode) to stimulate specific regions of one's brain. Research studies have shown that the application of tDCS on the leg area of the motor cortex can help to increase the motor evoked potential in the lower limb muscles [13]. Also, the application of tDCS at the primary and supplementary motor areas of the brain have been reported to affect the gait pattern of post-stroke patients [14], [15]. Specifically, Tahtis et al. [15] showed that bi-cephalic tDCS, with anode placed over the ipsilesional lower limb primary motor cortex and the cathode placed over the contralesional leg motor cortex, can bring clinical improvement

in the gait functionality of post-stroke patients. In the other study, Manji et al. [14] applied tDCS with anode placed in the front of 'Cz' (10/20 EEG montage) and the cathode placed at the inion improved gait speed (10-meter walk test [16]) and applicative walking ability (Timed-Up-and-Go [17]). Here, given the proximity of the representation of lower limbs in the primary motor cortex area, it is critical to ensure that the stimulation delivered using such montage was specific to the targeted lower limb [18],[10]. Specifically, the presumptive clinical applications of lower-limb tDCS need to take into account the unaffected contralesional hemisphere that produces inter-hemispheric inhibition where computational modeling can be used [18],[10].

Although the above-mentioned research studies focusing on the lower limb representation in the primary motor cortex have been promising, yet, it may also be important to investigate the role of cerebellar tDCS (ctDCS) [19] for post-stroke gait rehabilitation [20] since "the motor cortex retains what the cerebellum learns." Here, unlike the primary motor cortex stimulation that may increase the retention of newly learned visuomotor skills, ctDCS can facilitate motor adaptation during repetitive movements for gait rehabilitation [19]. Indeed, Zandvliet [20] showed that contra-lesional anodal cerebellar tDCS could improve standing balance performance; however, exploration of the dose is necessary. In this study, we aimed to investigate the lobular dosing of ctDCS based on two ctDCS montages, which were optimized using a computational pipeline [21]. Since the cerebellum plays an important role in balance and coordination, which are critical to gait recovery, as evidenced by TMS study [22], so it is postulated that ctDCS may also contribute towards improving the gait and balance of post-stroke patients. Here, the cerebellum can help in gait and posture by predicting the sensory output of motor commands and correcting the commands using a spatiotemporal interpretation of one's surroundings [23]. So, the function of the cerebellum is 'to build internal models that predict the sensory outcome of motor commands and correct motor commands through internal feedback [23]' based on the rehabilitation training. Prior works have shown that the cerebellum aids visually-guided limb movement and facilitates learning limb movement trajectories [24], [25], which is crucial for post-stroke gait rehabilitation.

Given the crucial role of the cerebellum in balance and gait, we aimed to investigate the effects of ctDCS on the post-stroke overground gait performance using regression analysis of the electric field distribution with the behavioral outcome [26]. Specifically, multivariate regression analysis can relate the changes in the balance and gait measures to the lobular electric field distribution due to ctDCS along cerebellar functional gradients [27]. With this motivation, we conducted this study to investigate the effects of ctDCS of the dentate nuclei and the leg lobules VII-IX on balance and overground gait ability of chronic stroke survivors. Based on our prior works [26], we optimized

 doi:10.20944/preprints202006.0338.v1

the ctDCS electrode montage, where our goal was to target cerebellar regions related to dentate nuclei and the lower-limb representation (cerebellar lobules VII-IX). The dentate nucleus is involved in the planning, initiating, and modifying voluntary movements as well as cognition. For regression analysis, the lobular electric field strength was proposed as a predictor of the changes in the gait parameters due to ctDCS intervention, which is based on our prior work on ctDCS effects on post-stroke standing balance [26]. So, the objectives of the current study were (i) evaluation of the acceptability of ctDCS by chronic stroke survivors, (ii) investigation of the effects of ctDCS on balance, clinical gait measures, as well as its regression analysis using the quantitative gait-related indices, (iii) investigation of the differential effects of the two ctDCS montages on balance, clinical gait measures and quantitative gait-related indices. In this study, we used our low-cost in-house built wearable gait characterizer [28] that can quantify gait performance in terms of Step Length [29], Walk Ratio [30], Gait Stability Ratio [31], and Symmetry Index [32]. The rest of the paper is organized as follows: Section II elaborates on the materials and methods used in our study, Section III presents the results, which is followed by the discussion and conclusion in Section IV.

II. Materials and Methods

Our wearable experimental setup comprised of (i) the Gait Quantification Shoe [28] (i.e., gait characterizer), and (ii) the wireless ctDCS cap, as shown in Figure 1. The Gait Quantification Shoe characterized one's gait parameters during overground walking. The ctDCS intervention was evaluated with the Gait Quantification Shoe to investigate the effects of ctDCS on the gait of chronic post-stroke hemiplegic patients recruited by convenience sampling from collaborating hospitals.

i. Study Participants

The hemiplegic stroke survivors, who (i) were aged between 18 and 90 years, (ii) could walk independently for at least 10 meters, (iii) could provide informed and written consent, and (iv) could understand instruction from the experimenter were contacted. Twelve post-stroke male subjects (P1-P12, Mean (SD) = 46(±13) years) were selected for the study (see Table 1) from fourteen volunteers. Here, volunteers who underwent any recent surgery or were in the acute phase of stroke were excluded from the study. Written informed consent was obtained from each subject, and the multi-center research protocol for this study was approved by the All India Institute of Medical Sciences, New Delhi, India Institutional Review Board (IEC-129/07.04.2017), and Indian Institute of Technology Gandhinagar, India Institutional Review Board (IEC/2019-20/4/UL/046).

ii. Gait Quantification Shoe

Preprints (www.preprints.org) | NOT PEER-REVIEWED | Posted: 28 June 2020 doi:10.20944/preprints202006.0338.v1

In this study, we aimed to quantify one's gait in terms of gait-related indices by recording gait events using a pair of instrumented shoe [28]. Figure 1 shows the wearable device, namely the Gait Quantification Shoes ($Gait_{Shoe}$ *henceforth*) [28], that was used in this study to record one's gait events. The $Gait_{Shoe}$ consisted of insoles instrumented with force-sensitive resistors (FSRs) that were placed below the greater toe, lateral heel and medial heel positions of each shoe to detect one's gait events, e.g., heel-strike, toe-off, etc. These gait events were used to compute different gait-related indices, e.g., Step Length [29], Walk Ratio [30], Gait Stability Ratio [31], and Symmetry Index [32], etc. The $Gait_{Shoe}$ was capable of transmitting the data wirelessly to a data logger computer for subsequent offline analysis.

[Place Figure 1 Here]

a. *Computation of Step Length*

Step Length is the distance between two successive contralateral heel-strikes during gait. We wanted to explore the implication of ctDCS on one's Step Length since this can be an essential indicator of the functional gait ability of hemiplegic post-stroke patients [29]. Here, we computed the average Step Length using the average Step Time (recorded by the $Gait_{Shoe}$) and the average Walking Speed. The Step Time was measured by the $Gait_{Shoe}$ from the time interval between two successive heel-strike events of contralateral legs. One's Walking Speed (during the overground walk) was computed from the time taken to walk through a pre-defined distance. Subsequently, the Step Length was calculated using Eq. (1). Finally, the Normalized Step Length was computed using the individualized height information [28] (Eq. (2)).

Step Length= Step Time * Walking Speed ……..(1)

Normalized Step Length = Step Length/Height……..…….(2)

b. *Computation of Gait Stability Ratio*

The Gait Stability Ratio (GSR) depends on one's Cadence (steps/sec) and Walking Speed (m/sec) [28]. The GSR is a good indicator of balance deficits in older adults [31]. The GSR takes into account the changes in one's Walking Speed that can influence one's Step Length. Here, a decrease in GSR might indicate increased double support time during one's walk, thereby inferring an increase in dynamic stability. The GSR was computed using Eq. (3).

Gait Stability Ratio= Cadence/Walking Speed …….(3)

c. *Computation of Walk Ratio*

Preprints (www.preprints.org) | NOT PEER-REVIEWED | Posted: 28 June 2020 doi:10.20944/preprints202006.0338.v1

The Walk Ratio (WR) [30] can describe a relation between one's Step Length and Cadence during walking. Importantly, WR is invariant during different speeds, uneven surface conditions, but is affected by dual task-condition [33]. The Walk Ratio was computed using Eq. (4).

Walk Ratio= Cadence/ Step Length ……(4)

d. Computation of Symmetry Index

The Symmetry Index (SI) is a measure of the extent to which one makes symmetrical use of both legs during walking [32] - smaller the value of SI, the better is the gait symmetry. One of the distinctive characteristics of post-stroke gait is the impaired gait symmetry, particularly in hemiplegic patients [34]. Here, we computed the SI using the %stance phase (of a gait cycle) measured using the $Gait_{Shoe}$ while considering the %stance for each of the left (X_L) and right legs (X_R). The SI was calculated using Eq. (5).

$SI= ((X_L-X_R) / 0.5 * (X_L+X_R)) *100$ ……..……(5)

[Place Figure 2 Here]

iii. Optimization of the Electrode Montage (age-specific computational modeling of ctDCS)

We used age-specific MRI templates that were obtained online at https://jerlab.sc.edu/projects/neurodevelopmental-mri-database/ with the permission of Dr. John Richards. The data comprised of average T1-weighted MRI for the head and brain and segmenting priors for gray matter (GM), white matter (WM), and cerebrospinal fluid (CSF). For this, we chose the age group that matched the age of our subjects for this study. A Realistic volumetric Approach to Simulate Transcranial Electric Stimulation (ROAST) [35] was used to create a tetrahedral volume mesh of the head. ROAST used SPM12("SPM - Statistical Parametric Mapping") to segment the head and brain. After segmentation, five tissues were identified for the tetrahedral volume mesh, namely, Scalp, Skull, Cerebrospinal Fluid (CSF), Gray Matter (GM), and White Matter (WM). These different brain tissues for the volume mesh were modeled as different volume conductors for Finite Element Analysis (FEA) in the ROAST. Here, isotropic conductivity used for the different brain tissues [36] were (in S/m): Scalp=0.465; Skull=0.01; CSF=1.654; GM=0.276; WM=0.126. For further details on the head modeling, please refer to our prior works [21], [26].

Preprints (www.preprints.org) | NOT PEER-REVIEWED | Posted: 28 June 2020 doi:10.20944/preprints202006.0338.v1

In this study, the Electric Field (EF) distribution was modeled for two different ctDCS montages for each subject's age-specific head model created from MRI templates (https://jerlab.sc.edu/projects/neurodevelopmental-mri-database/). The boundary condition was set as 2mA injection current (Neumann boundary condition) with the following electrode configurations from our prior work where we performed ctDCS optimization [26]:

a) **Optimized configuration for dentate stimulation** [26]: 3.14cm^2 disc anode was PO10h (10/5 EEG system), and 3.14cm^2 disc cathode was placed at PO9h (10/5 EEG system) for ctDCS with 2mA direct current.

b) **Optimized configuration for leg lobules VII-IX stimulation** [26]: 3.14cm^2 disc anode was Exx8 (electrodes defined by ROAST using "unambiguously illustrated (UI) 10/5 system" [37]), and 3.14cm^2 disc cathode was placed at Exx7 (defined by ROAST) for ctDCS with 2mA direct current.

In all the simulations, the voxel size was considered as 1mm^3. The contralesional anode and cathode injected the specified amount of current (source) in the volume conductor, i.e., the head model. Finite Element Analysis (FEA) was conducted on each head model to compute the ctDCS induced EF in the brain tissues. The electric field was computed at all the voxels (voxel size 1mm^3) of the cerebellar lobules defined by the cerebellar electric field distribution was normalized using spatially unbiased atlas for the cerebellum and brainstem (SUIT) [38]. Subsequently, the cerebellar lobular electric field distribution was found using SUIT [38], and T1-weighted images were fitted to the SUIT template of the human cerebellum in SPM12 ("SPM - Statistical Parametric Mapping": https://www.fil.ion.ucl.ac.uk/spm/software/spm12/). The cerebellar mask was visually checked in MRIcron, and the non-linear deformation was then applied to each EF image. The volume of the cerebellar lobules, defined by the SUIT atlas [38], was used for the extraction of the lobular EF distribution. Also, we customized SUIT codes to extract the left and the right dentate EF distribution.

iv. Experimental Setup and Data Analysis

Overground gait and balance evaluation were performed based on Timed-Up-and-Go (TUG) [17] and Berg Balance Score (BBS) [39] before and after the ctDCS intervention. Figure 1 shows the experimental setup for the clinical study in a low resource setting. The ctDCS setup consisted of a wireless STARSTIM 8 stimulator (Neuroelectrics, Spain). The study required a commitment of about 30 minutes from each participant.

a. Cerebellar tDCS intervention

Based on our prior work [26], 15 minutes of 2mA bilateral ctDCS was delivered in a repeated measure single-blind crossover design using either of the two bipolar montages with a circular (1cm radius) contralesional anode. The

Preprints (www.preprints.org) | NOT PEER-REVIEWED | Posted: 28 June 2020 doi:10.20944/preprints202006.0338.v1

electrode locations were based on the ROAST toolbox [35], and "unambiguously illustrated (UI) 10/5 system" [37]; 1. PO9h – PO10h, and 2. Exx7 – Exx8. Overground quantitative and clinical gait evaluation was performed before and after the ctDCS intervention to compute a percent normalized change measures, (POST-PRE)x100/(POST+PRE).

b. Experimental setup for overground gait analysis

The experimental setup for the overground gait analysis consisted of (i) 10 m long straight pathway (overground) marked with start and end lines, (ii) data-logger computer, and (iii) a pair of $Gait_{Shoes}$. In a repeated measure crossover design to compare the two ctDCS montages, we investigated the effects of ctDCS on one's gait characteristics during the overground walk. Once the participant arrived at the study hall, they were asked to sit and relax for about 5 minutes. Then, the experimenter explained to the participant what he was expected to do in the study as well as the risks. After informed consent, the baseline clinical measures, TUG, and BBS were recorded. Then, the experimenter helped the participant to wear the $Gait_{Shoe}$ [28]. Subsequently, the experimenter prepared the participant for ctDCS by placing the neoprene cap combined with a battery-driven wireless stimulator, Starstim 8 (Neuroelectrics, Spain), and the gel-based electrodes. The participants were informed that they could discontinue from the study in case of any discomfort.

Once the participant was ready to start the study, they were asked to walk on a 10m long straight path (overground) marked with a start and stop lines at their self-selected comfortable speed, and the participant's overground Walking Speed ($Speed_{OG}$) was computed. After this, the participant was asked to sit and relax on a chair for about 5 mins. Subsequently, ctDCS was administered in a repeated measure single-blind crossover design using one of the two ctDCS montages for 15 minutes at the rest condition with a dosage of 2 mA [26]. Following this, the participant repeated the 10m overground walk, followed by an assessment of the clinical gait and balance measures (TUG and BBS). The gait performance of the post-stroke participants was quantified using $Gait_{Shoe}$ in terms of the gait-related indices, as described earlier. Therefore, the post-stroke participants performed two trials of the overground walk, pre, and post ctDCS intervention, at their self-selected walking speed while wearing the $Gait_{Shoe}$, as illustrated in Figure 2. We also evaluated the acceptability of the ctDCS intervention in post-stroke subjects where we collected subjective feedback from the post-stroke participants prior to (Pre_{tDCS}), during ($Active_{tDCS}$), and post ($Post_{tDCS}$) application of ctDCS.

c) Statistical analysis and the partial least squares regression

Preprints (www.preprints.org) | NOT PEER-REVIEWED | Posted: 28 June 2020 doi:10.20944/preprints202006.0338.v1

Two-sided Wilcoxon rank-sum test was performed at the 5% significance level on the percent normalized change measures, $(\mathrm{POST}-\mathrm{PRE})\frac{100}{(\mathrm{POST}+\mathrm{PRE})}$ for the null hypothesis that the two ctDCS montages led to the same percent normalized change in the quantitative gait parameters from the same continuous distributions with equal medians. Also, Wilcoxon signed-rank test was conducted to find any change in the percent normalized change measures $(\mathrm{POST}-\mathrm{PRE})\frac{100}{(\mathrm{POST}+\mathrm{PRE})}$ due to ctDCS intervention for the null hypothesis that data comes from a distribution whose median is zero at the 5% significance level. Multivariate regression analysis was conducted to relate the changes in the balance and gait measures to the lobular electric field distribution due to ctDCS montages. Here, multicollinearity can occur when independent variables (predictors) are correlated. We have presented principal component regression analysis for multivariate linear regression of the lobular electric field distribution as the predictor with the behavioral outcomes as the response variables [26]. The goal is to extract the relation between electric field distribution and the behavioral effects of ctDCS where Partial Least Squares (PLS) is a promising multivariate statistical technique that can combine the information about the variances of both the predictors and the responses, while also considering the correlations among them [40]. In this study, we applied partial least squares regression approach to analyze the associations between the lobular electric field distribution as the predictor with the gait outcome measures as the response variables. Although statistical inference is the strength of PLSR approach using computational cross-validation methods (e.g., jackknife, bootstrap) [40]; however, we will apply PLS as a correlation technique in this study. The matrix of correlations between the lobular electric field distribution as the predictor with the gait outcome measures as the response variables is subjected to the singular value decomposition that results in the singular vectors called saliences. The lobular electric field distribution as the predictor with the gait outcome measures as the response variables can be projected onto their respective saliences, which creates latent variables that are linear combinations of the original variables. Here, PLS searches for latent variables that express the largest amount of information common to both the lobular electric field distribution as the predictor and the gait outcome measures as the response variables. This is a fixed-effect model where the results can only be interpreted with respect to the current data sets from this study. In this study, PLS analysis was performed on the percent normalized change measures, $(\mathrm{POST}-\mathrm{PRE})\frac{100}{(\mathrm{POST}+\mathrm{PRE})}$ of gait indices from the $\mathrm{Gait}_{\mathrm{shoe}}$ as the response variable, where the lobular electric field distribution for both the montages across all the subjects (found after centering the data and then singular value decomposition) was the predictor.

Preprints (www.preprints.org) | NOT PEER-REVIEWED | Posted: 28 June 2020 doi:10.20944/preprints202006.0338.v1

III. Results:

i. Acceptability of ctDCS

Once the cap with the electrodes and the portable tDCS device was placed on the participant's head, we obtained Pre_{tDCS} feedback from the participant to understand whether they were comfortable with the neoprene cap. Two subjects, P8 and P11, had challenges with the fitting of the ctDCS cap and the gel electrodes on the scalp, so they left the study. The rest of the 10 participants expressed that they were comfortable wearing the ctDCS cap with gel electrodes. The Pre_{tDCS} baseline feedback was followed by the feedback after the administration of the ctDCS, i.e., the $Active_{tDCS}$. Except two subjects who left the study at the baseline (Pre_{tDCS}) stage, none of the ten participants expressed any discomfort with the ctDCS intervention (at $Active_{tDCS}$); and, they reported a minor tingling sensation on the scalp for the first few seconds which was tolerable. After the application of ctDCS, the $Post_{tDCS}$ verbal feedback revealed that none of the participants had any adverse effects, such as a sensation of tissue burning, nausea, headache, etc. Also, no skin reddening (at the location of electrodes) of the scalp was noticed. From this, we concluded that post-stroke patients in this study could tolerate the ctDCS with 3.14cm^2 disc gel electrodes at 2mA direct current.

ii. *Effects of ctDCS on Gait-related Indices measured using the* $Gait_{Shoe}$

Effects of ctDCS on post-stroke overground gait were quantified using the $Gait_{Shoe}$ that measured gait-related indices, e.g., Step Length, Gait Stability Ratio, Walk Ratio, and Symmetry Index. Also, the mean lobular electric field strengths for all the 10 participants using their age-specific head model was found for both the ctDCS montages, dentate ctDCS and leg (lobules VII-IX) ctDCS, as shown in Figure 3. Figure 3a shows that the leg ctDCS also affected the dentate nuclei besides the targeted lobules VII-IX at a comparable electric field strength (0.1 V/m), while the Figure 3b shows that the dentate ctDCS primarily affected the dentate nuclei at greater than 0.2 V/m electric field strength. These results are based on computational modeling using subject's age-matched healthy MRI templates where four post-stroke subjects were left hemiplegic and the remaining six right hemiplegics, as shown in Table 1.

[Place Figure 3 Here]

Figure 4 shows the percent normalized change measures, $(\mathrm{POST}-\mathrm{PRE})\frac{100}{(\mathrm{POST}+\mathrm{PRE})}$, in the gait parameters across the 10 participants due to the two ctDCS montages. The distribution shown in the violin plots in Figure 4 was found to be mostly not normal. Therefore, non-parametric two-sided Wilcoxon rank sum test at 5% significance level was used to find the difference in the effects between the two ctDCS montages where statistically significant effect was

Preprints (www.preprints.org) | NOT PEER-REVIEWED | Posted: 28 June 2020 doi:10.20944/preprints202006.0338.v1

found for 'Step Time Affected Leg' (p=0.0257) and '%Stance Time Unaffected Leg' (p=0.0376) while the montage specific effect was found to be insignificant for 'Normalised Step length Affected side' (p=0.6776), 'Normalised Step length Unaffected side' (p=0.1859), 'Walk Ratio Affected side' (p=0.5205), 'Walk Ratio Unaffected side' (p=0.7337), 'Gait Stability Ratio' (p=0.7913), 'Symmetry Index' (p=0.9097), 'Stride Time Affected Leg' (p=0.4727), 'Stride Time Unaffected Leg' (p=0.3847), 'Step Time Unaffected Leg' (p=0.7913), '%Stance Time Affected Leg' (p=0.4274), '%Swing Time Affected Leg' (p=0.5205), '%Swing Time Unaffected Leg' (p=0.0539), '%Single Support Time Affected Leg' (p=0.1212), '%Single Support Time Unaffected Leg' (p=0.3075), 'Cadence' (p=0.0890). When the effects from both the ctDCS montages are combined across subjects then the Wilcoxon signed rank test found significant ctDCS effects at 10% significance level for 'Normalised Step length Affected side' (p=0.1) and 'Gait Stability Ratio' (p=0.0569) while the ctDCS effects were found to be insiginificant for 'Normalised Step length Unaffected side' (p=0.2471), 'Walk Ratio Affected side' (p=0.1790), 'Walk Ratio Unaffected side' (p=0.3703), 'Symmetry Index' (p=0.1169), 'Stride Time Affected Leg' (p=0.2959), 'Stride Time Unaffected Leg' (p=0.3317), 'Step Time Affected Leg' (p=0.1454), 'Step Time Unaffected Leg' (p=0.3135), '%Stance Time Affected Leg' (p=0.3135), '%Stance Time Unaffected Leg' (p=0.9108), '%Swing Time Affected Leg' (p=0.3317), '%Swing Time Unaffected Leg' (p=1), '%Single Support Time Affected Leg' (p=0.9405), '%Single Support Time Unaffected Leg' (p=0.2959), 'Cadence' (p=0.7089).

[Place Figure 4 Here]

The effects of the two montages of the ctDCS were found similar across ten subjects for most gait parameters. Figure 5a shows a reasonable correlation between fitted and observed responses using partial least squares (PLS) analysis with the mean lobular electric field strength as the predictors, which was confirmed by the R^2 statistic = 0.6574. Residuals passed the Lilliefors test for two-sided goodness-of-fit for normality. Choosing the number of components in a PLS model is a critical step where greater than 60% of the variance in the response variables (percent normalized change in gait parameters) was explained by the first ten components of the predictor variables (mean lobular electric field strength), as shown in Figure 5b.

[Place Figure 5 Here]

Preprints (www.preprints.org) | NOT PEER-REVIEWED | Posted: 28 June 2020 doi:10.20944/preprints202006.0338.v1

Furthermore, the loadings of the latent variables on the response variables (percent normalized change in gait parameters) and the predictor variables (mean lobular electric field strength) are shown in Figures 6a and 6b, respectively. Here, we found that the cerebellar lobules, Vermis VIIIb, Ipsilesional IX, Vermis IX, Ipsilesional X, were related by the component 2 positively to the 'Step Time Affected Leg' ($p=0.0257$) and '%Stance Time Unaffected Leg' ($p=0.0376$), that showed significant effects between the two ctDCS montages using two-sided Wilcoxon rank-sum test. Also, the cerebellar lobules, Vermis VIIIb, Ipsilesional IX, Vermis IX, Ipsilesional X, were related by the component 2 negatively to the '%Swing Time Unaffected Leg' ($p=0.0539$), '%Single Support Time Affected Leg' ($p=0.1212$). Figure 6c shows that the cerebellar lobules, Vermis VIIIb, Ipsilesional IX, Vermis IX, Ipsilesional X, had the lowest difference in their mean lobular electric field strength between the two ctDCS montages for all 10 subjects.

[Place Figure 6 Here]

iii. *Effects of ctDCS on the Balance and Gait related Clinical Measures*

The results from the clinical assessment of the 10-meter walk test, TUG, and the BBS showed that there was a small improvement in the duration of the 10m walk test and the TUG test (reduction was about 2.5% and 4%, respectively), which indicated an improved walking speed. Also, we found an improvement (about 5%) in the BBS score; however, the improvement in the TUG and BBS scores were similar across both the ctDCS montages.

IV Discussion and Conclusion:

In this study, we investigated the effects of two different ctDCS montages on overground gait parameters. Although the montages were computationally optimized for targeting the dentate nuclei and the leg representations in the cerebellum; however, both the ctDCS montages resulted in higher than 0.1V/m electric field strength at the dentate nuclei, as shown in Figure 3. In fact, we found it challenging to avoid affecting the dentate nucleus, the largest of the deep cerebellar nuclei when targeting leg lobules VII-IX. In this study, ctDCS intervention was found to affect the BBS, TUG, and the quantitative gait parameters, 'Normalised Step length Affected side' ($p=0.1$) and 'Gait Stability Ratio' ($p=0.0569$) based on the Wilcoxon signed rank test at 10% significance level. A decrease in 'Gait Stability Ratio' was found which indicates an increase in dynamic stability. Also, ctDCS montage specific effects were found for the 'Step Time Affected Leg' ($p=0.0257$) and '%Stance Time Unaffected Leg' ($p=0.0376$) using two-sided Wilcoxon rank-sum test at 5% significance level, as shown in Figure 4. These changes can be attributed to the ctDCS

Preprints (www.preprints.org) | NOT PEER-REVIEWED | Posted: 28 June 2020 doi:10.20944/preprints202006.0338.v1

electric field strength since individual changes in the quantitative gait parameters across both the montages were found to be correlated to the mean electric field strength in the lobules based on partial least squares (PLS) regression analysis (see Figure 5). The loadings of the latent variables found from PLS analysis (see Figure 6) for the response variables (percent normalized change in gait parameters) and the predictor variables (mean lobular electric field strength) showed that the mean electric field strength at the posterior cerebellar lobules, Vermis VIIIb, Ipsilesional IX, Vermis IX, Ipsilesional X, were primarily related to the 'Step Time Affected Leg' and '%Stance Time Unaffected Leg.' Both the ctDCS montages used ipsilesional cathode where 'Step Time Affected Leg' ($p=0.0257$) and '%Stance Time Unaffected Leg' ($p=0.0376$) showed significant effects between the two ctDCS montages at 5% significance level. The ipsilesional cathode effects may be related to the cerebellar-brain inhibition, where prior work in healthy subjects showed robust effects of cathodal ctDCS after-effects on cerebellar-brain inhibition [41]. Such effects of cerebellar-brain inhibition on the contralesional leg motor cortex can be compared with the results from Tahtis et al. [15] where bi-cephalic tDCS with cathode placed over the contralesional leg motor cortex, i.e., postulated reduction of the excitability of the contralesional leg motor cortex, improved the gait functionality of post-stroke patients. Also, posterior vermis has been shown to be related to the performance on tandem walking [42], where lobule X was found essential in the vestibular system [43] while motor and somatosensory activation have been linked to the lobule VIIIb [44]. This is postulated to be related to the significant effect of ctDCS on the 'Gait Stability Ratio' which has been shown to be an indicator of balance during walking [31]. Moreover, step length variability during tandem walking has been related to the lesion in the lobules VIIIb and IX [25] that we did not investigate in this study; however, ctDCS effects were found for the 'Normalised Step length Affected side.' These posterior cerebellar lobules lobules VIIIb, IX, and X were affected by comparable mean electric field strength across the two ctDCS montages, as shown in Figure 6c, which is may have led to comparable balance and gait related behavioral outcomes across the two ctDCS montages. We found that PLS analysis can be an effective technique for regression modeling to understand the relation between the electric field distribution and the behavioral effects where PLS results can also be generalized (i.e., to create a random effect model) using inferential analytical approach [40] when a larger dataset is available.

Clinical literature shows a crucial role of the cerebellum in coordinating voluntary movements (e.g., walking) and maintaining one's balance [45]. In this current study, the cerebellum was intact so that the ctDCS was performed to ameliorate deficits in the rest of the motor network in the cerebrum. Random-effects modeling of the cumulative effect size by Oldrati and Schutter [46] showed that anodal and cathodal ctDCS were effective in changing motor- and

cognitive-related behavioral performance in healthy volunteers. However, the polarity of ctDCS was not predictive of the direction of the behavioral changes in healthy volunteers [46]. Nevertheless, robust effects of the cathodal ctDCS after-effects have been found on cerebellar-brain inhibition [41], which may be related to the behavioral changes. However, the clinical applicability of ctDCS in improving the functional gait ability remains under-explored due to a diversity of ideas on cerebellar involvement in the movement and the inter-subject variability in the ctDCS effects [47]. We postulate based on cerebellar ataxia studies [48] that ctDCS may also be feasible in some cases of cerebellar damage. Here, besides neuroimaging guided subject-specific head modeling, portable neuroimaging may be able to capture the immediate response of the ctDCS on the cerebrum [49] that may be used for individual dosing.

Our preliminary findings in this study are encouraging; however, this study had certain limitations. Specifically, one of the limitations was the small sample size of chronic post-stroke participants with heterogeneous conditions. Therefore, the low statistical power has a reduced chance of detecting a true effect [50], so this study can be considered as a feasibility study. Also, the convenience sampling in this study was biased since all of our participants were male hemiplegics, with four being left hemiplegic and the remaining six right hemiplegics. In the future, we plan to extend our study involving more post-stroke participants from both the genders. Although contralesional anode was used for bi-hemispheric ctDCS, the electrode locations were not optimized for individual cases. So, "one-size-fits-all" montage was used across the subjects that were optimized based on the subject's age-specific head model from an MRI template that did not have any lesions. This limited any subject specific inferences using the partial least squares analysis considering that the post-stroke participants had heterogeneous lesion conditions in the cerebrum. The cerebellum was intact in all the subjects in this study; however, heterogeneous lesion locations in the cerebrum need further investigation, especially in the non-responders, where multi-block or multi-table PLS can integrate one or more of these varieties in a common analysis [40]. In the future, we also plan to segregate the extended pool of post-stroke participants based on the portable neuroimaging of the ctDCS response [49] for such multi-table PLS analysis.

In conclusion, both the ctDCS montages targeted the dentate nuclei, and the "one-size-fits-all" ctDCS intervention was limited to a single session, which improved gait and balance performance with low statistical power, and no significant difference was found between the montages for most gait parameters. Nevertheless, the quantitative gait parameters across both the montages were found to be correlated to the mean lobular electric field strength, which can be considered a preliminary step towards understanding the underlying mechanisms of ctDCS for gait rehabilitation.

V. Acknowledgment

The authors would like to thank the Department of Science and Technology India, Visvesvaraya Fellowship, and Indian Institute of Technology Gandhinagar for their support to carry out this work. Authors are grateful to Dr. M. V. Padma Srivastava at the All India Institute of Medical Sciences, Delhi, for her support with the clinical study. The authors are also grateful to physiotherapists at Govt. Spine Institute and B1 physiotherapy ward at Civil Medical Hospital, Ahmedabad, and All India Institute of Medical Sciences, Delhi. This research was funded by the Indian Ministry of Human Resource Development (MHRD)'s Scheme for Promotion of Academic and Research Collaboration (SPARC), grant number 2018–2019/P721/SL, and Indian Department of Health Research, Project Code No. N1761.

VI. Authors' contributions

DS, AD, UL designed the research and the experimental protocol; DS analyzed the behavioral data under the supervision of UL while ZR performed computational head modeling, statistical and partial least squares regression analysis under the supervision of AD; DS, ZR, AD, UL conducted review and editing; AD, UL provided project administration and resources; and DS, ZR wrote the paper.

VII. References

1. Johnson CO, Nguyen M, Roth GA, Nichols E, Alam T, Abate D, et al. Global, regional, and national burden of stroke, 1990–2016: a systematic analysis for the Global Burden of Disease Study 2016. The Lancet Neurology. Elsevier; 2019;18:439–58.

2. Duncan PW, Zorowitz R, Bates B, Choi JY, Glasberg JJ, Graham GD, et al. Management of Adult Stroke Rehabilitation Care: a clinical practice guideline. Stroke. 2005;36:e100-143.

3. Hendricks HT, van Limbeek J, Geurts AC, Zwarts MJ. Motor recovery after stroke: a systematic review of the literature. Arch Phys Med Rehabil. 2002;83:1629–37.

4. Dobkin BH. Rehabilitation after Stroke. N Engl J Med. 2005;352:1677–84.

5. Belda-Lois J-M, Mena-del Horno S, Bermejo-Bosch I, Moreno JC, Pons JL, Farina D, et al. Rehabilitation of gait after stroke: a review towards a top-down approach. J Neuroeng Rehabil. 2011;8:66.

6. Rogers LM, Madhavan S, Roth H, Stinear JW. Transforming neurorehabilitation of walking following stroke: the promise of non-invasive brain stimulation--a review. Restor Neurol Neurosci. 2011;29:507–16.

7. Vaz PG, Salazar AP da S, Stein C, Marchese RR, Lukrafka JL, Plentz RDM, et al. Noninvasive brain stimulation combined with other therapies improves gait speed after stroke: a systematic review and meta-analysis. Top Stroke Rehabil. 2019;26:201–13.

8. Kang N, Lee RD, Lee JH, Hwang MH. Functional Balance and Postural Control Improvements in Patients With Stroke After Noninvasive Brain Stimulation: A Meta-analysis. Arch Phys Med Rehabil. 2020;101:141–53.

9. Nitsche MA, Doemkes S, Karaköse T, Antal A, Liebetanz D, Lang N, et al. Shaping the Effects of Transcranial Direct Current Stimulation of the Human Motor Cortex. Journal of Neurophysiology. American Physiological Society; 2007;97:3109–17.

10. Foerster AS, Rezaee Hassan Abadi Z, Paulus W, Nitsche M, Dutta A. Effects of cathode location and the size of anode on anodal transcranial direct current stimulation over the leg motor area in healthy humans. Front Neurosci [Internet]. 2018 [cited 2018 Jun 20];12. Available from: https://www.frontiersin.org/articles/10.3389/fnins.2018.00443/abstract

11. Schlaug G, Renga V, Nair D. Transcranial direct current stimulation in stroke recovery. Arch Neurol. 2008;65:1571–6.

12. Nitsche MA, Paulus W. Excitability changes induced in the human motor cortex by weak transcranial direct current stimulation. J Physiol (Lond). 2000;527 Pt 3:633–9.

13. Jeffery DT, Norton JA, Roy FD, Gorassini MA. Effects of transcranial direct current stimulation on the excitability of the leg motor cortex. Exp Brain Res. 2007;182:281–7.

14. Manji A, Amimoto K, Matsuda T, Wada Y, Inaba A, Ko S. Effects of transcranial direct current stimulation over the supplementary motor area body weight-supported treadmill gait training in hemiparetic patients after stroke. Neurosci Lett. 2018;662:302–5.

15. Tahtis V, Kaski D, Seemungal BM. The effect of single session bi-cephalic transcranial direct current stimulation on gait performance in sub-acute stroke: A pilot study. Restor Neurol Neurosci. 2014;32:527–32.

16. Cheng DK, Nelson M, Brooks D, Salbach NM. Validation of stroke-specific protocols for the 10-meter walk test and 6-minute walk test conducted using 15-meter and 30-meter walkways. Topics in Stroke Rehabilitation. Taylor & Francis; 2020;27:251–61.

17. Persson CU, Danielsson A, Sunnerhagen KS, Grimby-Ekman A, Hansson P-O. Timed Up & Go as a measure for longitudinal change in mobility after stroke – Postural Stroke Study in Gothenburg (POSTGOT). J Neuroeng Rehabil. 2014;11:83.

18. Otal B, Dutta A, Foerster Á, Ripolles O, Kuceyeski A, Miranda PC, et al. Opportunities for Guided Multichannel Non-invasive Transcranial Current Stimulation in Poststroke Rehabilitation. Front Neurol [Internet]. 2016 [cited 2018 Jun 23];7. Available from: https://www.ncbi.nlm.nih.gov/pmc/articles/PMC4764713/

19. Galea JM, Vazquez A, Pasricha N, Orban de Xivry J-J, Celnik P. Dissociating the Roles of the Cerebellum and Motor Cortex during Adaptive Learning: The Motor Cortex Retains What the Cerebellum Learns. Cereb Cortex. 2011;21:1761–70.

20. Zandvliet SB, Meskers CGM, Kwakkel G, van Wegen EEH. Short-Term Effects of Cerebellar tDCS on Standing Balance Performance in Patients with Chronic Stroke and Healthy Age-Matched Elderly. Cerebellum. 2018;17:575–89.

21. Rezaee Z, Dutta A. Cerebellar Lobules Optimal Stimulation (CLOS): A Computational Pipeline to Optimize Cerebellar Lobule-Specific Electric Field Distribution. Front Neurosci [Internet]. 2019 [cited 2019 Jun 15];13. Available from: https://www.frontiersin.org/articles/10.3389/fnins.2019.00266/full#B5

22. Koch G, Bonnì S, Casula EP, Iosa M, Paolucci S, Pellicciari MC, et al. Effect of Cerebellar Stimulation on Gait and Balance Recovery in Patients With Hemiparetic Stroke. JAMA Neurol. 2019;76:170–8.

459 23. Shadmehr R, Krakauer JW. A computational neuroanatomy for motor control. Exp Brain Res. 2008;185:359–81.

460 24. Morton SM, Bastian AJ. Cerebellar contributions to locomotor adaptations during splitbelt treadmill walking. J
461 Neurosci. 2006;26:9107–16.

462 25. Ilg W, Timmann D. Gait ataxia--specific cerebellar influences and their rehabilitation. Mov Disord.
463 2013;28:1566–75.

464 26. Rezaee Z, Kaura S, Solanki D, Dash A, Srivastava MVP, Lahiri U, et al. Deep Cerebellar Transcranial Direct
465 Current Stimulation of the Dentate Nucleus to Facilitate Standing Balance in Chronic Stroke Survivors—A Pilot
466 Study. Brain Sciences. 2020;10:94.

467 27. Guell X, Schmahmann JD, Gabrieli JD, Ghosh SS. Functional gradients of the cerebellum. Bostan A, Ivry RB,
468 editors. eLife. 2018;7:e36652.

469 28. Solanki D, Lahiri U. Design of Instrumented Shoes for Gait Characterization: A Usability Study With Healthy
470 and Post-stroke Hemiplegic Individuals. Front Neurosci [Internet]. 2018 [cited 2020 May 2];12. Available from:
471 https://www.ncbi.nlm.nih.gov/pmc/articles/PMC6062939/

472 29. Awad LN, Palmer JA, Pohlig RT, Binder-Macleod SA, Reisman DS. Walking speed and step length asymmetry
473 modify the energy cost of walking after stroke. Neurorehabil Neural Repair. 2015;29:416–23.

474 30. Murakami R, Otaka Y. Estimated lower speed boundary at which the walk ratio constancy is broken in healthy
475 adults. J Phys Ther Sci. 2017;29:722–5.

476 31. Cromwell RL, Newton RA. Relationship between balance and gait stability in healthy older adults. J Aging Phys
477 Act. 2004;12:90–100.

478 32. Viteckova S, Kutilek P, Svoboda Z, Krupicka R, Kauler J, Szabo Z. Gait symmetry measures: A review of
479 current and prospective methods. Biomedical Signal Processing and Control. 2018;42:89–100.

480 33. Bogen B, Moe-Nilssen R, Ranhoff AH, Aaslund MK. The walk ratio: Investigation of invariance across walking
481 conditions and gender in community-dwelling older people. Gait Posture. 2018;61:479–82.

482 34. Ofran Y, Karniel N, Tsenter J, Schwartz I, Portnoy S. Functional Gait Measures Prediction by Spatiotemporal
483 and Gait Symmetry in Individuals Post Stroke. J Dev Phys Disabil. 2019;31:611–22.

484 35. Huang Y, Datta A, Bikson M, Parra LC. ROAST: An Open-Source, Fully-Automated, Realistic Volumetric-
485 Approach-Based Simulator For TES. Conf Proc IEEE Eng Med Biol Soc. 2018;2018:3072–5.

486 36. Windhoff M, Opitz A, Thielscher A. Electric field calculations in brain stimulation based on finite elements: an
487 optimized processing pipeline for the generation and usage of accurate individual head models. Hum Brain Mapp.
488 2013;34:923–35.

489 37. Jurcak V, Tsuzuki D, Dan I. 10/20, 10/10, and 10/5 systems revisited: Their validity as relative head-surface-
490 based positioning systems. NeuroImage. 2007;34:1600–11.

491 38. Diedrichsen J. A spatially unbiased atlas template of the human cerebellum. Neuroimage. 2006;33:127–38.

492 39. Blum L, Korner-Bitensky N. Usefulness of the Berg Balance Scale in Stroke Rehabilitation: A Systematic
493 Review. Phys Ther. Oxford Academic; 2008;88:559–66.

494 40. Krishnan A, Williams LJ, McIntosh AR, Abdi H. Partial Least Squares (PLS) methods for neuroimaging: A
495 tutorial and review. NeuroImage. 2011;56:455–75.

496 41. Batsikadze G, Rezaee Z, Chang D-I, Gerwig M, Herlitze S, Dutta A, et al. Effects of cerebellar transcranial
497 direct current stimulation on cerebellar-brain inhibition in humans: A systematic evaluation. Brain Stimulation:
498 Basic, Translational, and Clinical Research in Neuromodulation [Internet]. 2019 [cited 2019 Jun 15];0. Available
499 from: https://www.brainstimjrnl.com/article/S1935-861X(19)30201-3/abstract

500 42. Bastian AJ, Mink JW, Kaufman BA, Thach WT. Posterior vermal split syndrome. Ann Neurol. 1998;44:601–10.

501 43. Stoodley CJ, Schmahmann JD. Functional topography in the human cerebellum: a meta-analysis of
502 neuroimaging studies. Neuroimage. 2009;44:489–501.

503 44. Stoodley CJ, Schmahmann JD. Evidence for topographic organization in the cerebellum of motor control versus
504 cognitive and affective processing. Cortex. 2010;46:831–44.

505 45. Morton SM, Tseng Y-W, Zackowski KM, Daline JR, Bastian AJ. Longitudinal Tracking of Gait and Balance
506 Impairments in Cerebellar Disease. Mov Disord. 2010;25:1944–52.

507 46. Oldrati V, Schutter DJLG. Targeting the Human Cerebellum with Transcranial Direct Current Stimulation to
508 Modulate Behavior: a Meta-Analysis. Cerebellum. 2018;17:228–36.

509 47. Manto M, Bower JM, Conforto AB, Delgado-García JM, da Guarda SNF, Gerwig M, et al. Consensus Paper:
510 Roles of the Cerebellum in Motor Control—The Diversity of Ideas on Cerebellar Involvement in Movement.
511 Cerebellum. 2012;11:457–87.

512 48. Maas RPPWM, Toni I, Doorduin J, Klockgether T, Schutter DJLG, van de Warrenburg BPC. Cerebellar
513 transcranial direct current stimulation in spinocerebellar ataxia type 3 (SCA3-tDCS): rationale and protocol of a
514 randomized, double-blind, sham-controlled study. BMC Neurol [Internet]. 2019 [cited 2020 Jun 26];19. Available
515 from: https://www.ncbi.nlm.nih.gov/pmc/articles/PMC6610834/

516 49. Rezaee Z, Ranjan S, Solanki D, Bhattacharya M, Srivastava MP, Lahiri U, et al. Functional near-infrared
517 spectroscopy in conjunction with electroencephalography of cerebellar transcranial direct current stimulation
518 responses in the latent neurovascular coupling space – a chronic stroke study. bioRxiv. Cold Spring Harbor
519 Laboratory; 2020;2020.05.24.113928.

520 50. Button KS, Ioannidis JPA, Mokrysz C, Nosek BA, Flint J, Robinson ESJ, et al. Power failure: why small sample
521 size undermines the reliability of neuroscience. Nature Reviews Neuroscience. Nature Publishing Group;
522 2013;14:365–76.

523

Preprints (www.preprints.org) | NOT PEER-REVIEWED | Posted: 28 June 2020 doi:10.20944/preprints202006.0338.v1

524 **Tables**

Table 1: Participant Characteristics (greyed subjects are dropouts)

Patient ID	Age Group (years)	Height (cm)	Weight (kilograms)	Post Stroke Period (years)	Affected Limb
P1	40-44	167	73	2	Right
P2	50-54	171	70	3	Right
P3	35-39	180	60	1	Left
P4	35-39	165	80	1	Right
P5	30-34	176	94	1	Right
P6	45-49	162	60	2	Left
P7	50-54	167	83	1	Left
P8	70-74	163	76	6	Right
P9	40-44	164	60	3	Right
P10	45-49	167	70	2	Left
P11	60-64	161	47	3	Right
P12	35-39	165	76	2	Right

525
526
527
528
529
530
531
532
533
534
535
536
537
538

 doi:10.20944/preprints202006.0338.v1

539 **Figure captions**

540 Figure 1: Experimental setup

541 Figure 2: Block diagram for the experimental protocol

542 Figure 3: a) Violin plot of the mean lobular electric field strength (V/m) across 10 participants for the optimized
543 configuration for leg lobules VII-IX stimulation. b) Violin plot of the mean lobular electric field strength (V/m) across
544 10 participants for the optimized configuration for dentate stimulation. Violin plot allowed visualization of the
545 distribution of the data and its probability density where the box plot (with median, interquartile range, upper adjacent
546 value, lower adjacent value) is combined with the probability density placed on each side.

547 Figure 4: a) Violin plot of the mean % change in the gait parameters across 10 participants due to ctDCS optimized
548 for leg lobules VII-IX stimulation. b) Violin plot of the mean % change in the gait parameters across 10 participants
549 due to ctDCS optimized for dentate stimulation. Violin plot allowed visualization of the distribution of the data and
550 its probability density where the box plot (with median, interquartile range, upper adjacent value, lower adjacent value)
551 is combined with the probability density placed on each side.

552 Figure 5: a) The scatter plot shows a reasonable correlation between fitted and observed responses after partial least
553 squares (PLS) regression for all the response variables (percent normalized change in gait parameters). b) Greater than
554 60% of the variance in the response variables (percent normalized change in gait parameters) was explained by the
555 first ten components of the predictor variables (mean lobular electric field strength).

556 Figure 6: Partial least squares (PLS) component loadings. a) loadings of the latent variables of the response variables
557 (percent normalized change in gait parameters) where the components are in the x-axis. b) loadings of the latent
558 variables of the predictor variables (mean lobular electric field strength) where the components are in the x-axis. c)
559 contrast in mean lobular electric field strength (V/m) for 10 participants between the dentate and the leg lobules VII-
560 IX ctDCS montages. 'Contra' is contralesional and 'Ipsi' is ipsilesional.

561

 doi:10.20944/preprints202006.0338.v1

562 **Figures**

563

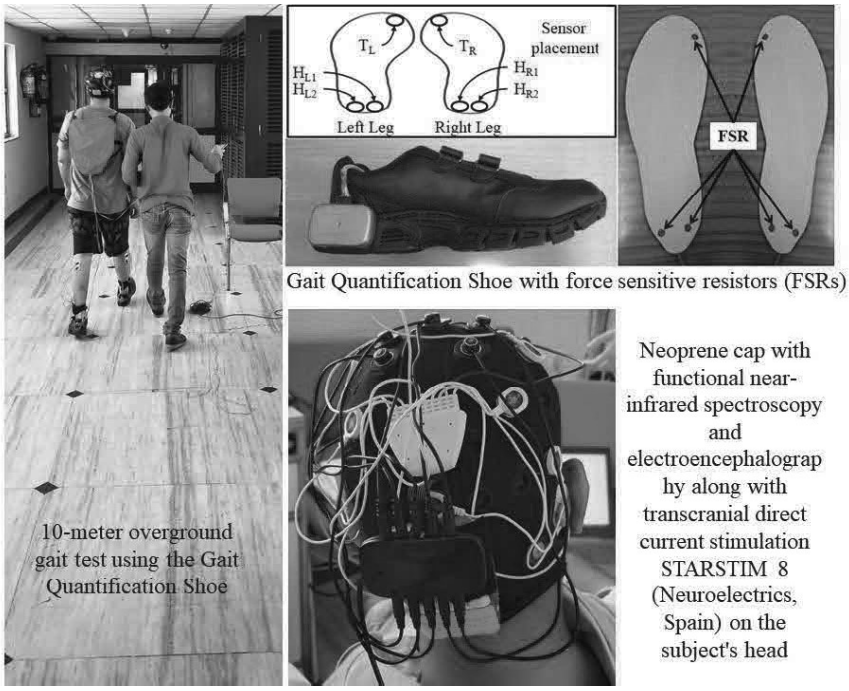

Figure 1: Experimental setup

564

565

566

567

568

569

570

 doi:10.20944/preprints202006.0338.v1

571

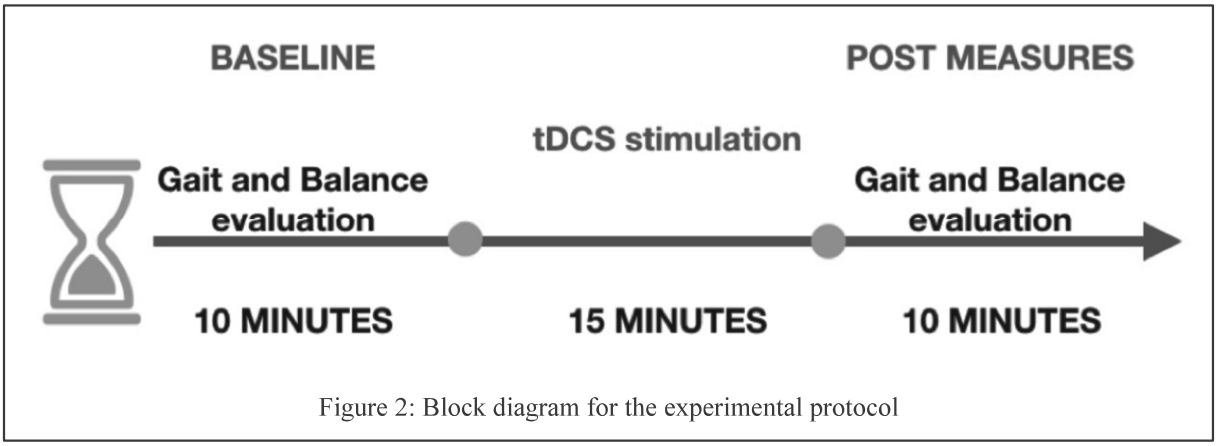

Figure 2: Block diagram for the experimental protocol

572

573

Preprints (www.preprints.org) | NOT PEER-REVIEWED | Posted: 28 June 2020 doi:10.20944/preprints202006.0338.v1

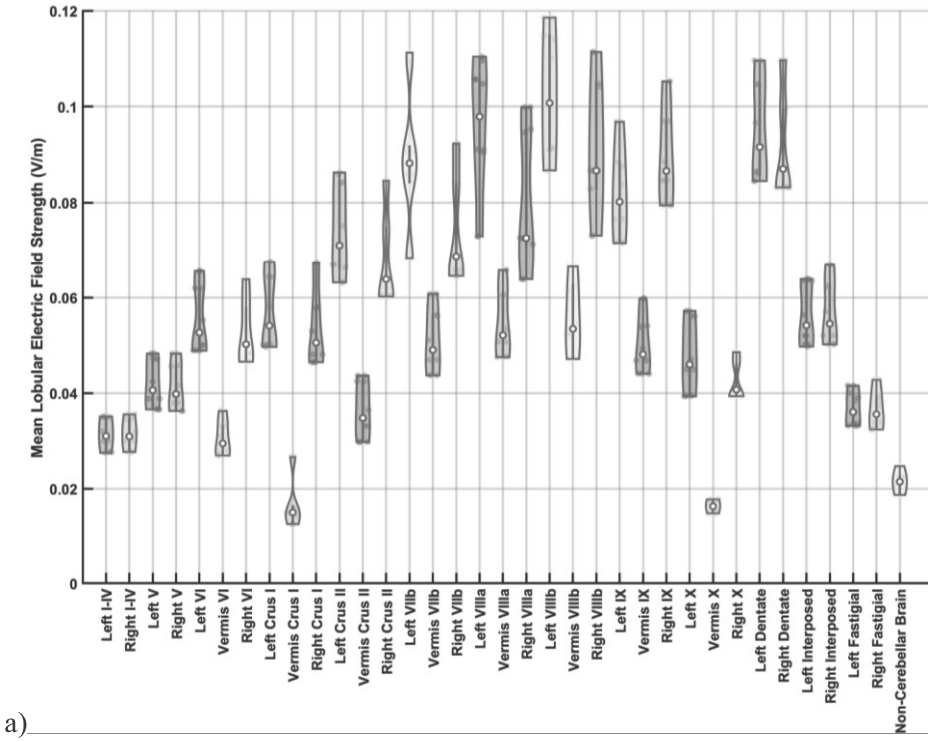

a)

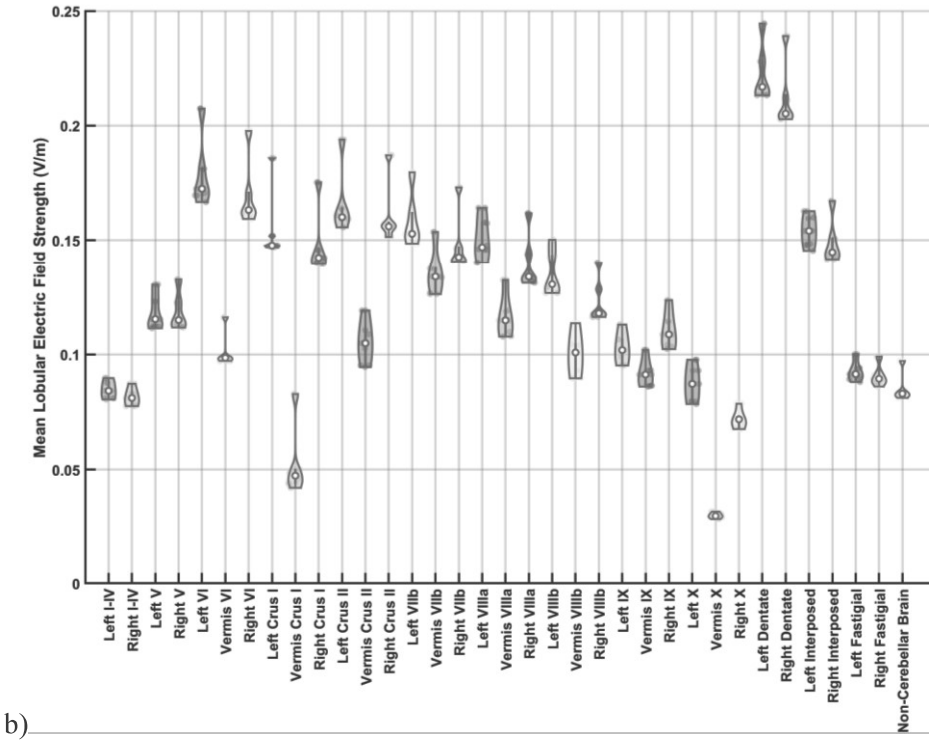

b)

Figure 3: a) Violin plot of the mean lobular electric field strength (V/m) across 10 participants for the optimized configuration for leg lobules VII-IX stimulation. b) Violin plot of the mean lobular electric field strength (V/m) across 10 participants for the optimized configuration for dentate stimulation. Violin plot allowed visualization of the distribution of the data and its probability density where the box plot (with median, interquartile range, upper adjacent value, lower adjacent value) is combined with the probability density placed on each side.

574

Preprints (www.preprints.org) | NOT PEER-REVIEWED | Posted: 28 June 2020 doi:10.20944/preprints202006.0338.v1

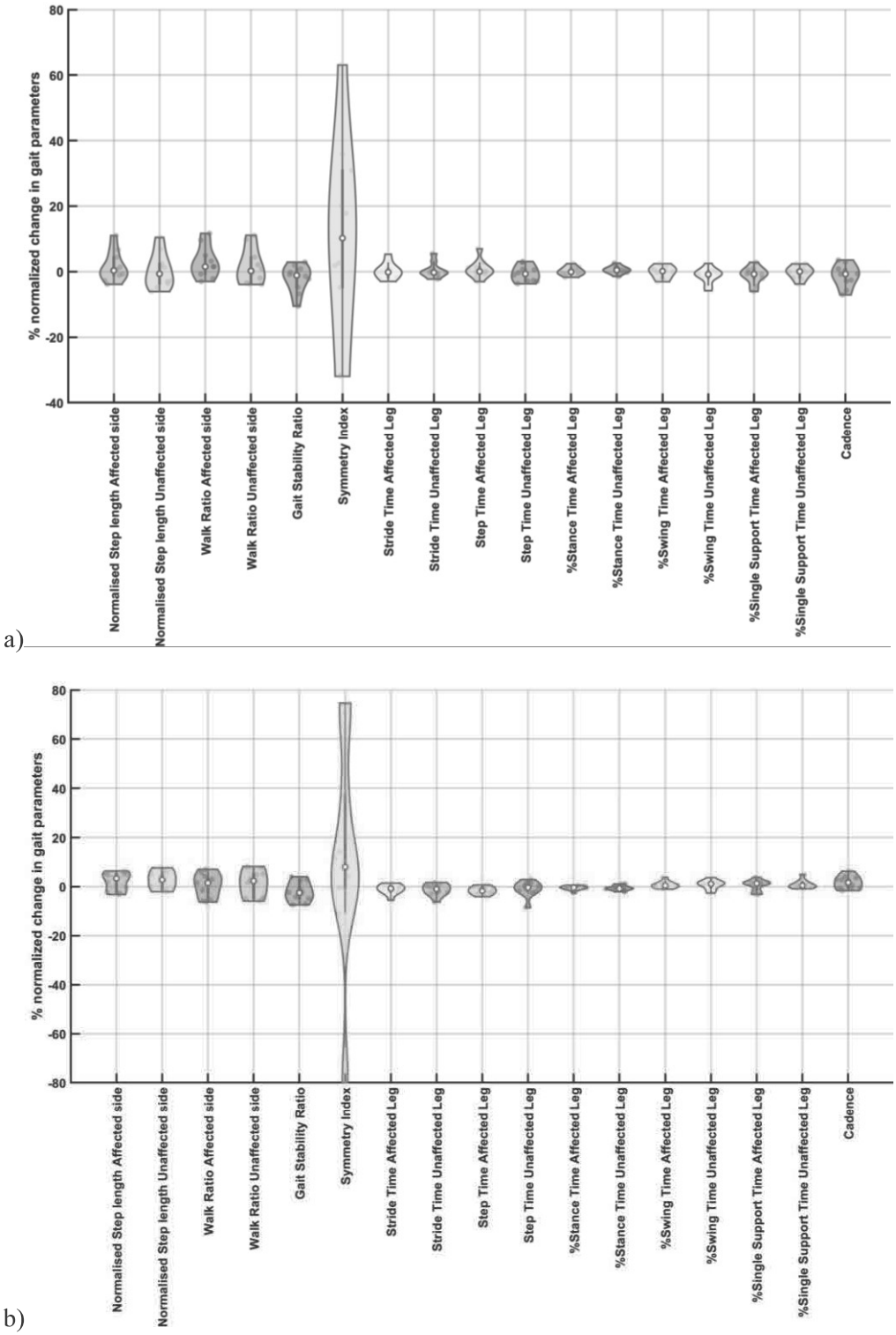

Figure 4: a) Violin plot of the mean % change in the gait parameters across 10 participants due to ctDCS optimized for leg lobules VII-IX stimulation. b) Violin plot of the mean % change in the gait parameters across 10 participants due to ctDCS optimized for dentate stimulation. Violin plot allowed visualization of the distribution of the data and its probability density where the box plot (with median, interquartile range, upper adjacent value, lower adjacent value) is combined with the probability density placed on each side.

575

Preprints (www.preprints.org) | NOT PEER-REVIEWED | Posted: 28 June 2020 doi:10.20944/preprints202006.0338.v1

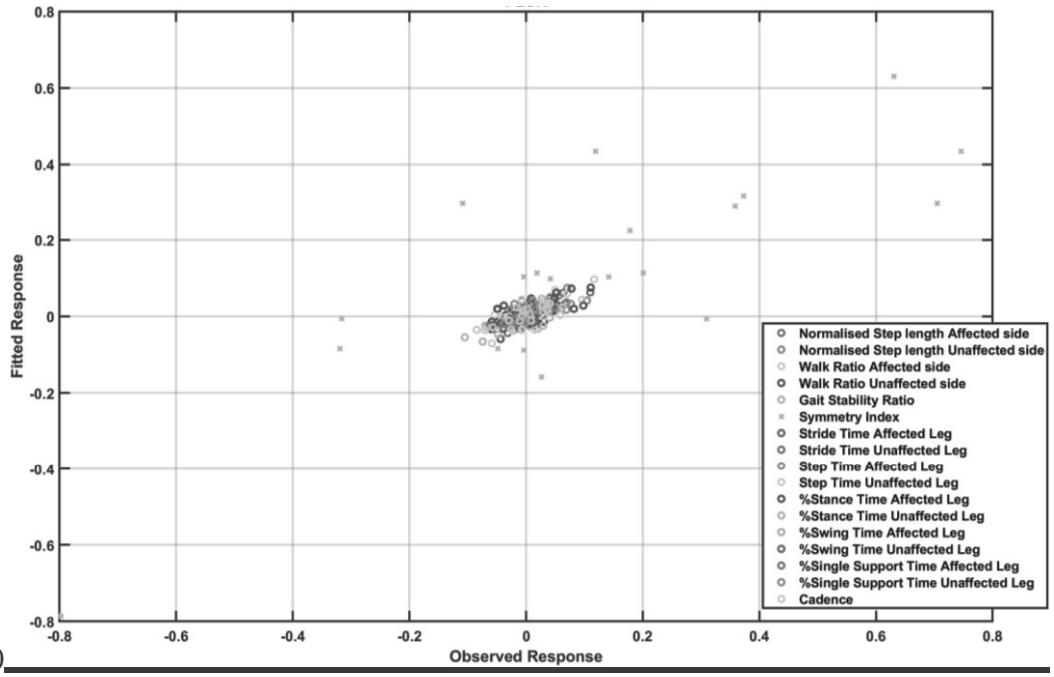

a)

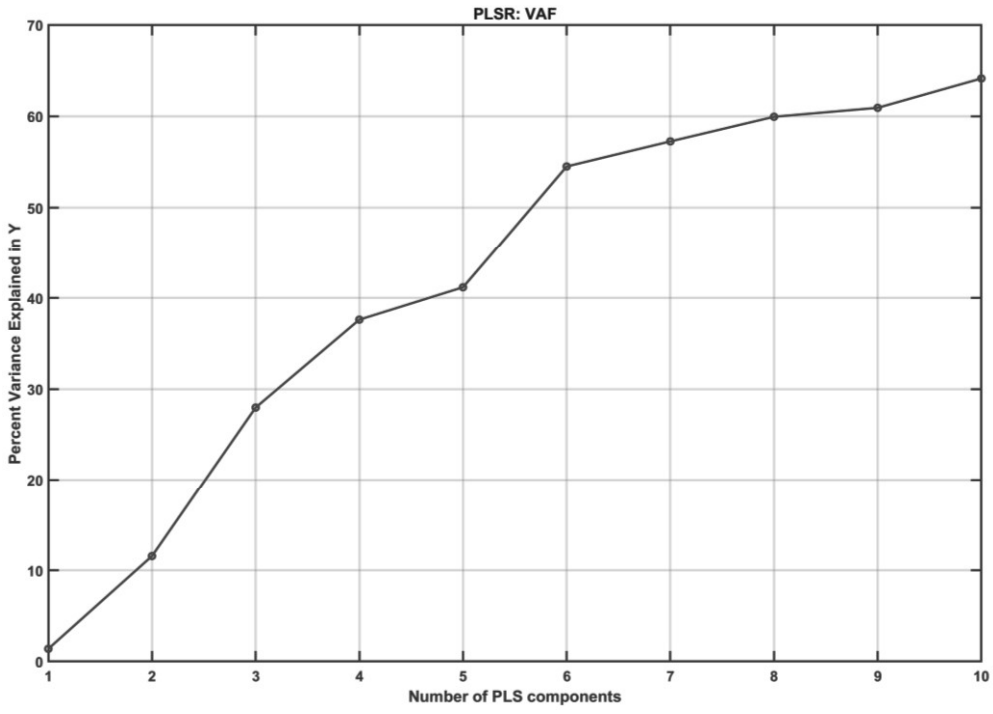

b)

Figure 5: a) The scatter shows a reasonable correlation between fitted and observed responses after partial least squares (PLS) regression for all the response variables (percent normalized change in gait parameters) . b) Greater than 60% of the variance in the response variables (percent normalized change in gait parameters) was explained by the first ten components of the predictor variables (mean lobular electric field strength).

576

577

Preprints (www.preprints.org) | NOT PEER-REVIEWED | Posted: 28 June 2020 doi:10.20944/preprints202006.0338.v1

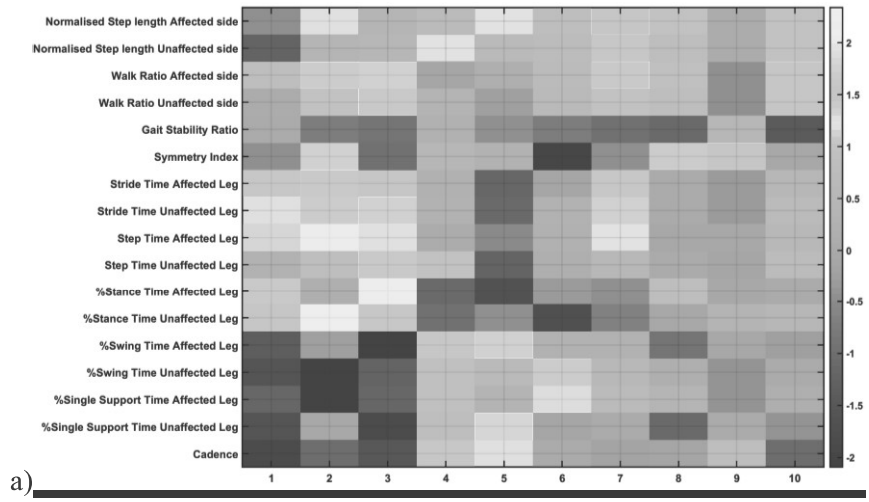

a)

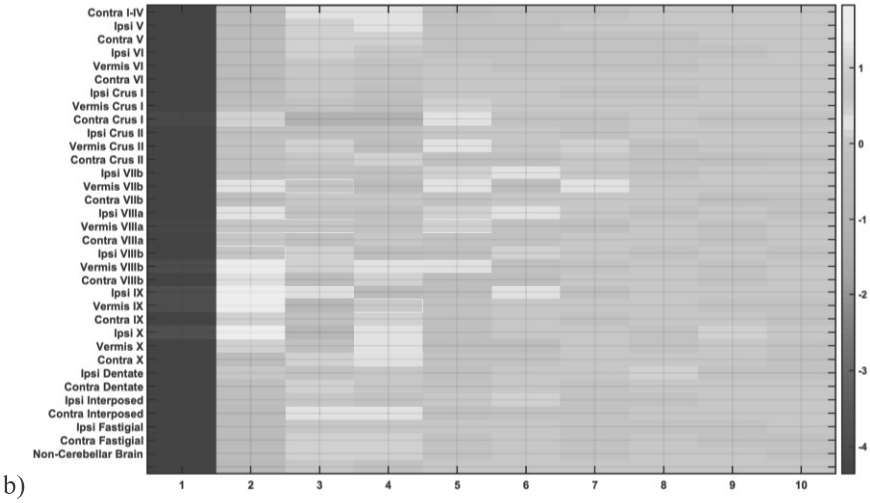

b)

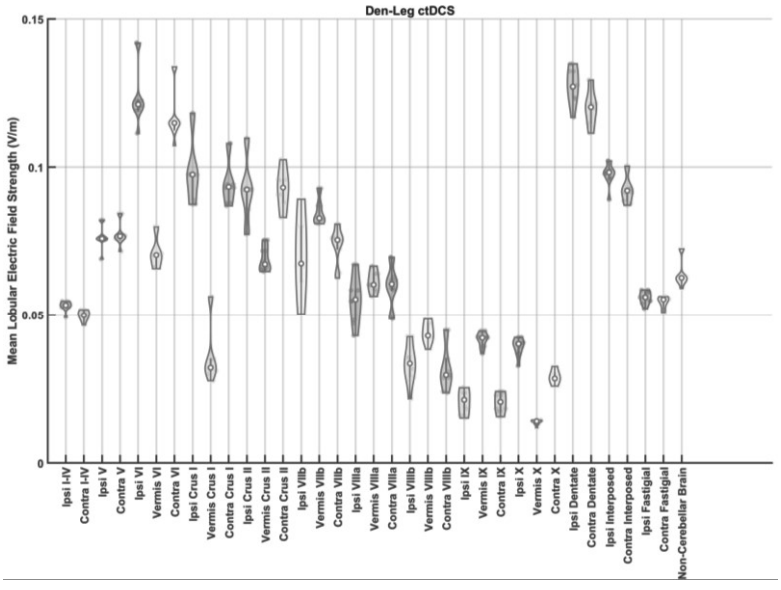

c)

Figure 6: Partial least squares (PLS) component loadings. a) loadings of the latent variables of the response variables (percent normalized change in gait parameters) where the components are in the x-axis. b) loadings of the latent variables of the predictor variables (mean lobular electric field strength) where the components are in the x-axis. c) contrast in mean lobular electric field strength (V/m) for 10 participants between the dentate and the leg lobules VII-IX ctDCS montages. 'Contra' is contralesional and 'Ipsi' is ipsilesional.